Hydrogen Generation from Thermochemical Water-Splitting Using Core-Shell Ni-Ferrite Nanoparticles

V.S. Amar, L. Garrett, J. Puszynski and R.V. Shende*

Department of Chemical and Biological Engineering,
South Dakota School of Mines & Technology,
Rapid City,SD 57701, USA, Rajesh.Shende@sdsmt.edu

ABSTRACT

During thermochemical water-splitting process for hydrogen generation, ferrite nanoparticles undergo significant grain growth that reduces their surface area and affect the porous morphology. Consequently, hydrogen volume generation diminishes with increase in thermochemical cycles. In order to mitigate the grain growth, we have encapsulated the ferrite nanoparticles with porous shell of thermally stable ceramic material. Ni-ferrite nanoparticles were synthesized using the sol-gel method and further utilized to prepare core-shell nanoparticles with ZrO_2 or Y_2O_3. As-prepared core-shell $NiFe_2O_4/ZrO_2$ nanoparticles were analyzed by powdered X-Ray diffraction, transmission electron microscopy (TEM) and BET specific surface area analyzer. TEM analysis indicated core-shell morphology with Ni-ferrite encapsulated inside ZrO_2 shell of average thickness of 6.12 nm. Core-shell Ni-ferrite/ZrO_2 nanoparticles were loaded in Inconel reactor and five consecutive thermochemical cycles were performed at 900^o– 1100^{o}C for hydrogen generation. The results indicated relatively steady hydrogen volume generation in multiple thermochemical cycles.

Keywords: hydrogen, thermochemical water-splitting, core-shell, $NiFe_2O_4/ZrO_2$.

1 INTRODUCTION

Hydrogen is high energy density fuel which can be effectively utilized in fuel cell systems for power generation [1]. It can be produced by electrolysis of water or steam reforming of hydrocarbons. However, traditional methods of hydrogen production [2-6] lead to CO_2 emission, which is believed to be affecting weather patterns [7]. A two-step thermochemical water-splitting [8] is a cleaner process for producing hydrogen at higher temperatures. In step-1 (regeneration), redox material is partially reduced at higher temperatures whereas in step-2 (water-splitting) partially reduced redox material scavenges oxygen from high temperature steam producing hydrogen. Consequently, oxygen and hydrogen are prduced in separate steps thus avoiding the formation of explosive mixture.

In our previous investigations [9, 10] we reported sol-gel synthesis of redox materials for hydrogen generation from thermochemical water-splitting process. In these investigations, we observed gradual decrease in hydrogen volume generation with increase in number of thermochemical cycles. In order for this technology to be industrially viable, it is imperative to produce steady hydrogen volume generation in multiple thermochemical cycles. To realize steady hydrogen volume generation, we investigated X-ray diffraction patterns and microstructures of redox nanoparticles after thermochemical water-splitting reaction. These investigations revealed no change in the phase composition for $NiFe_2O_4$ but grain growth. Increased grain growth will increase diffusional distance for oxygen transport through crystal lattice. Therefore, we believe that grain growth of Ni-ferrite nanoparticles should be controlled during thermal cycling to achieve steady hydrogen generation.

Recently, we attempted to mitigate grain growth of Ni-ferrite nanoparticles by mixing them with grain growth inhibitors such as ZrO_2, Y_2O_3, Al_2O_3 and YSZ *via* vortex or sonication [11,12]. Using $NiFe_2O_4/ZrO_2$ material, four consecutive thermochemical cycles were performed at water-splitting temperature of 900^{o}C. $NiFe_2O_4/ZrO_2$ powders prepared by ultrasonic mixing [11] and vortex mixing [12] produced H_2 volume of avg. 64.6 ml/g/cycle and 47.69 ml/g/cycle, respectively. These hydrogen generation volumes are still higher than avg. 36.42 ml/g/cycle generated by $NiFe_2O_4$. These results infer that higher H_2 volume generation using $NiFe_2O_4/ZrO_2$ mixture is partly due to the grain growth inhibition caused by ZrO_2 addition.

In this study, we attempted to encapsulate sol-gel derived Ni-ferrite nanoparticles inside ZrO_2 shell leading to the formation of core-shell nanoparticle morphology. These core-shell particles were characterized using powder X-ray diffraction, BET surface area analyzer and transmission electron microscopy (TEM), and utilized inside Inconel reactor where five consecutive thermochemical cycles were performed at 900^o-1100^{o}C for hydrogen generation.

2 EXPERIMENTAL

2.1 Ni-ferrite Nanoparticles

Calculated quantities of $NiCl_2.6H_2O$ and $FeCl_2.4H_2O$ were added in 1:2 (w/w) ratio in ethanol and sonicated for 90 min until visually clear solution was obtained. Gelation was

accomplished by the addition of propylene oxide. The gel was aged for 24 hours, dried at ~100°C and calcined as per the procedure outlined in our earlier investigation [9].

2.2 Core-shell Nanoparticles

As prepared sol-gel derived Ni-ferrite nanoparticles were dispersed in isopropanol and sonicated for 2 hours. To this dispersion, Pluronic P123 (10 wt% of Ni-ferrite) was added and sonication was further continued for 2 hours. Next, zirconium isopropoxide (70% in isopropanol) was added dropwise to the Ni-ferrite dispersion (25 wt%), which was sonicated for additional 2 hours. The addition of de-ionized water led to the gel formation. The gels were aged for 48 hours, dried at ~100°C for 1 hour and calcined at 600°C. The entire synthesis route for the core-shell nanoparticles is shown in Figure 1.

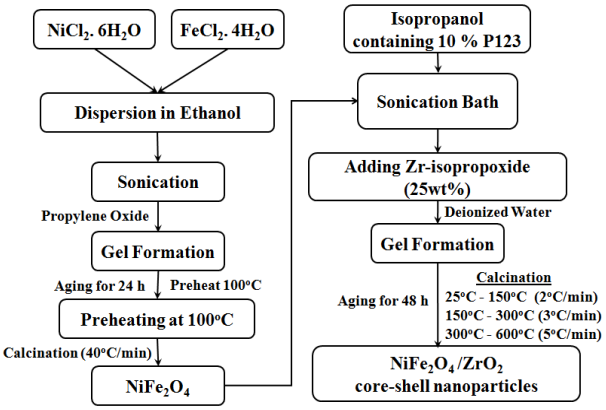

Figure 1: Sol-gel synthesis of Ni-ferrite/ZrO_2 core-shell nanoparticles.

2.3 Characterization of Nanoparticles

Ni-ferrite/ZrO_2 core-shell nanoparticles obtained after calcination were analyzed to determine phase purity and crystallographic properties using Rigaku Ultima plus X-ray diffractometer (XRD) equipped with Cu$K\alpha$ radiation (λ=1.5406 Å, 40 kV, 40 mA). The samples were analyzed in the range of $10^o \leq 2\theta \leq 90^o$ with the scanning speed of 2^o/min. The specific surface area (SSA) and the pore volume (P_v) of the core-shell nanoparticles were determined by using Micromeritics Gemini II – 2375 BET (Brunauer Emmett Teller) surface area analyzer. The core-shell morphology of the nanoparticles was studied using high resolution Hitachi H-7000 FA transmission electron microscope (HRTEM). To prepare samples for the TEM analysis, about 1 mg powdered sample was dispersed in ethanol containing 5wt% Pluronic P123 surfactant. 1-2 drops of dispersion were added to the carbon coated copper grid and plasma cleaned to remove the residual hydrocarbon impurities.

2.4 H_2 Generation Reactor Set-up

The experimental thermochemical water-splitting reactor set-up available in our laboratory has been previously reported elsewhere [10]. Ni-ferrite/ZrO_2 core-shell nanoparticles were loaded inside the Inconel tubular reactor, which was placed in the vertical split furnace (Carbolite Inc., USA). During the regeneration step, the redox material was heated at a temperature (T_{reg}) of 1100°C for 2 hours under the constant N_2 flow rate of 35 cm^3/min. The furnace temperature was reduced to 900°C to perform the water-splitting step. Deionized water vaporized at 500°C in a horizontal tube furnace (Carbolite Inc., USA) was fed into tubular packed bed reactor where the water splitting reaction was performed at 900°C. The concentration of the product gas stream was continuously monitored using hydrogen gas sensor (H2SCAN). After every water splitting step, the reactor was regenerated for 2 hours at 1100°C and cooled down again to 900°C to carry out additional water-splitting step. Five consecutive thermochemical cycles were performed at 900°-1100°C using the core-shell nanoparticles.

3 RESULTS AND DISCUSSION

The XRD pattern of the Ni-ferrite/ZrO_2 nanoparticles calcined at 600°C is shown in Figure 2. The charactacteristic peaks corresponding to 2θ reflections confirmed, $NiFe_2O_4$ spinel structure and these peak positions are in agreement with the published literature [9]. Three characteristic peaks observed at $2\theta = 30.22^o$, 50.39^o and 60.06^o corresponding to lattice planes of <111>, <220>, and <311>, respectively confirmed the presence of tetragonal ZrO_2. These 2θ reflections are in agreement with those reported in the literature [13] and consistent with ICDD pattern (JCPDS, No 17-0923 [14]).

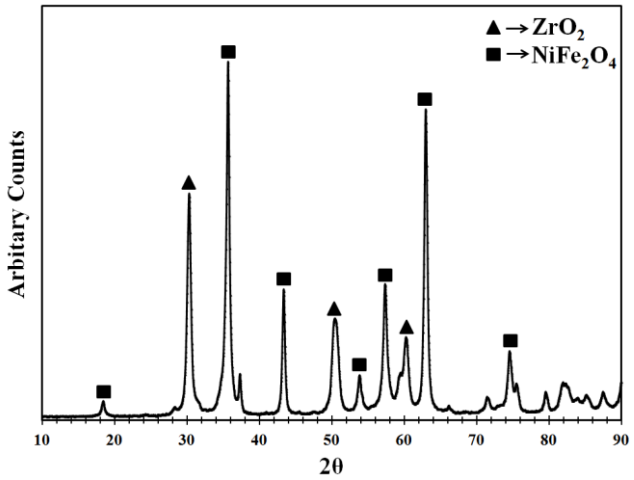

Figure 2: XRD pattern indicates $NiFe_2O_4$ and ZrO_2 crystalline phases in core-shell nanoparticles calcined at 600°C.

CTSI-Cleantech 2014, www.ct-si.org, ISBN 978-1-4822-5819-6

Accurately weighed 500 mg $NiFe_2O_4/ZrO_2$ nanoparticles were degassed at 200°C and analysed for their surface properties using BET (Brunauer-Emmet-Teller) surface area analyzer. The BET analysis showed specific surface area and pore volume of 30.70 m^2/g and 0.26 cm^3/g, respectively. The morphology of the $NiFe_2O_4/ZrO_2$ core-shell nanoparticles was characterized using Hitachi H-7000FA TEM as per the procedure described earlier in the Experimental section. Among several TEM images obtained, a representive TEM image is presented in Figure 3. The image shows core-shell morphology with several nanoparticles encapsulated inside the shell. The *d*-spacing of 0.48 nm oriented along the <111> plane for the particles residing inside the shell confirmed the presence of $NiFe_2O_4$ [15]. The TEM analysis of the shell indicated uniform amorphous coating of ZrO_2 of average thickness of 6.12 nm adhering to the $NiFe_2O_4$ nanoparticles confirming the core-shell morphology.

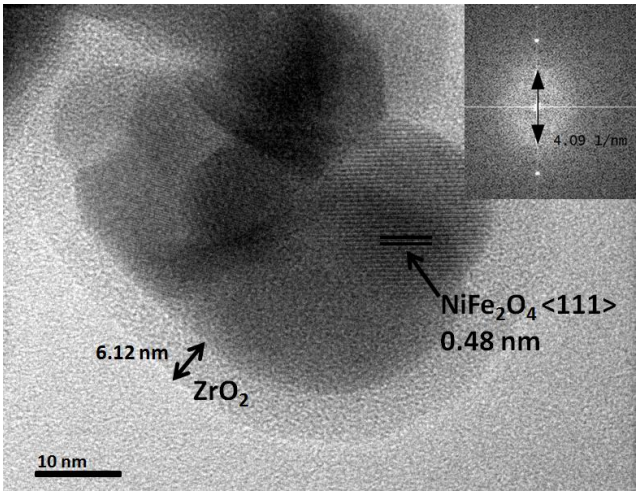

Figure 3: HRTEM image of $NiFe_2O_4/ZrO_2$ nanoparticles showing core-shell morphology.

$NiFe_2O_4/ZrO_2$ core-shell nanoparticles were loaded in Inconel tubular reactor and packed with raschig rings where regeneration and water splitting steps were performed at 1100°C and 900°C, respectively. The transient hydrogen profiles obtained during five consecutive thermochemical cycles are shown in Figure 4, where average hydrogen yield was observed as 2.45 ml/g/cycle at NTP conditions. The transient hydrogen profiles produced during multiple water-splitting steps indicate hydrogen volume generation values within ±10%. These results convey the notion that the grain growth of core-shell nanoparticles might have been mitigated during multiple thermochemical cycles. Thus, encapsulation of $NiFe_2O_4$ nanoparticles with porous ZrO_2 shell is found to be advantageous in terms of stabilizing hydrogen volume generation over multiple cycles. It is to be noted that the hydrogen generation ability of the core-shell nanoparticles is lower when compared to the $NiFe_2O_4$ nanoparticles [9]. This could be due to the agglomeration of $NiFe_2O_4$ nanoparticles inside the ZrO_2 shell, which would grow and sinter leading to decrease in specific surface area during thermal cycling. Consequently, higher diffisional resistance will limit scavenging of oxygen during water-splitting step. Currently we are improving synthesis methods to achieve monoparticulate core-shell nanoparticle morphology and investigating their hydrogen generation ability.

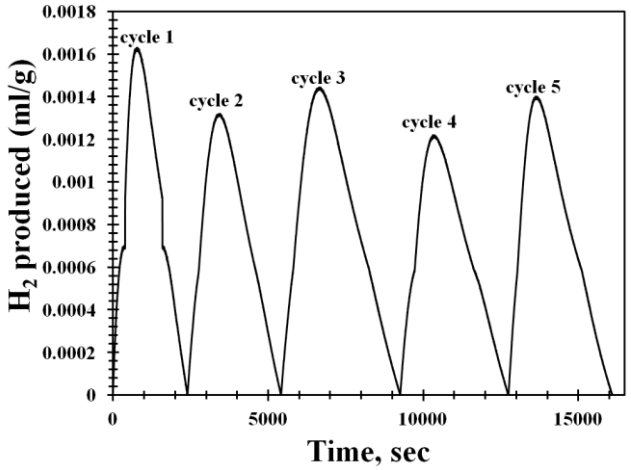

Figure 4: Transient H_2 profiles obtained during five thermochemical cycles where water splitting and regeneration steps were performed at 900°C and 1100°C, respectively using core-shell nanoparticles.

4 CONCLUSIONS

$NiFe_2O_4/ZrO_2$ core-shell nanoparticles were successfully synthesized by sol-gel technique using pluronic P123 surfactant. The TEM analysis confirmed the presence of amorphous ZrO_2 shell around a cluster of few $NiFe_2O_4$ nanoparticles. As synthesized core-shell nanoparticles were loaded in the Inconel reactor and five consecutive thermochemical cycles were performed with regeneration and water splitting steps at 1100°C and 900°C, respectively. The average H_2 volume generated during five thermochemical cycles was 2.45 ml/g/cycle. The transient hydrogen profiles suggest that the encapsulation of $NiFe_2O_4$ nanoparticles inside ZrO_2 shell is advantageous to some extent in stabilizing hydrogen volume generation over multiple cycles.

ACKNOWLEDGEMENTS

The authors gratefully acknowledge the financial support from the National Science Foundation, Grant No. CBET#1134570 and Chemical and Biological Engineering department at South Dakota School of Mines & Technology.

REFERENCES

[1] U. Bossel, "Does a Hydrogen Economy Make Sense?," Proceedings of the IEEE, 94, 1826-1837, 2006.

[2] P. L. Spath, and K. M Margaret, "Life Cycle Assessment of Hydrogen Production via Natural Gas Steam Reforming," National Renewable Energy Laboratory in Golden Colorado, 2000.

[3] J. P. Gomez, and J. L. G. Fierro, "New Catalytic Routes for Syngas and Hydrogen Production," Applied Catalysis A: General, 144, 7-57, 1996.

[4] D. Gray, and G. Tomlinson, "Hydrogen from Coal," Mitretek Technical Paper MTR, 31, 2002.

[5] Y. F. Wang, Y. S. You, C. H Tsai and L. C. Wang, "Production of Hydrogen by Plasma-Reforming of Methanol," International Journal of Hydrogen Energy, 35, 9637-9640, 2010.

[6] R. I. Kermode, "Hydrogen from Fossil Fuels," Hydrogen: Its Technology and Implications, 1, 61-115, 1977.

[7] R. M. Rotty, "Estimates of Seasonal Variation in Fossil Fuel CO_2 Emissions," Tellus B, 29B, 184-202, 1987.

[8] J. E. Funk, "Thermochemical Production of Hydrogen via Multistage Water Splitting Processes," International Journal of Hydrogen Energy, 1, 33-43, 1976.

[9] R. R. Bhosale, R. V. Shende, and J. A. Puszynski, "H_2 Generation from Thermochemical Water Splitting Using Sol-gel Derived Ni-ferrite," Journal of Energy and Power Engineering, 4, 27-38, 2010.

[10] R. R. Bhosale, R. V. Shende, and J. A. Puszynski, "Thermochemical Water-Splitting for H_2 Generation Using Sol-Gel Derived Mn-ferrite in a Packed Bed Reactor," International Journal of Hydrogen Energy, 37, 2924-2934, 2012.

[11] R. R. Bhosale, R. V. Shende, and J. A. Puszynski, "Sol-Gel Derived $NiFe_2O_4$ Modified with ZrO_2 for Hydrogen Generation from Solar Thermochemical Water-Splitting Reaction," MRS Proceedings, Cambridge University Press, 1387, 2012.

[12] X. Pasala, R. R. Bhosale, V. S. Amar, R. V. Shende, and J. A. Puszynski, "Thermally Stabilized Ferrite Nanoparticles for Hydrogen Generation from Thermochemical Water Splitting Reaction," Proceedings of AIChE Annual Meeting, 2012.

[13] J. Du, Y. Liu, G. Yao, Z. Hua, X. Long, and B. Wang, "Microstructure, Mechanical Properties, and Pyroconductivity of $NiFe_2O_4$ Composite Reinforced with ZrO_2 Fibers," Journal of Materials Engineering and Performance, 22, 1776-1782, 2013.

[14] T. N. Blanton, T. C. Huang, H. Toraya, C. R. Hubbard, S. B. Robie, D. Louer, H. E. Göbel, G. Will, R. Gilles, and T. Raftery, "JCPDS—International Centre for Diffraction Data Round Robin Study of Silver Behenate. A Possible Low-angle X-ray Diffraction Calibration Standard," Powder Diffraction, 10, 91-95, 1995.

[15] V. Šepelák, I. Bergmann, A. Feldhoff, P. Heitjans, F. Krumeich, D. Menzel, F. J. Litterst, S. J. Campbell, and K. D. Becker, "Nanocrystalline Nickel Ferrite, $NiFe_2O_4$: Mechanosynthesis, Nonequilibrium Cation Distribution, Canted Spin Arrangement, and Magnetic Behavior," The Journal of Physical Chemistry C, 111, 5026-5033, 2007.